

DRYING OF POROUS MATERIAL USING FINITE ELEMENT METHOD

H.N. SURESH¹, K. MURUGESAN², P.A. Aswatha NARAYANA³, and K.N. SEETHARAMU⁴

¹ P.E.S. College of Engineering, Mandya - 571 401, INDIA.

² KREC, Surathkal, INDIA

³ Indian Institute of Technology, Madras - 600 036, INDIA.

⁴ Universiti sains MALAYSIA, Tronoh, Perak campus, MALAYSIA.

ABSTRACT

Economy and rapidity are common to the drying of some industrial products and in some cases these products should be dried under some specific conditions necessary to preserve their quality. This is the case for a number of vegetable products and chemical substances whose chemical and textural integrity should not be impaired. During the brick drying process, heat and mass transfer takes place between the solid and the drying medium and moisture evaporation takes place within the solid due to capillary action and diffusion. In the present study, two-dimensional Navier-Stokes equations along with energy and concentration equations for the fluid coupled with energy and mass conservation equations for the solid are used to study the conjugate drying behavior. Whitaker's [1] continuum approach has been used to obtain the equation for liquid and vapour migration within the solid. A finite element analysis has been carried out using the Galerkin's weighted residual technique to solve the governing equations. The results have been analysed under free, forced and mixed convection environments and have been obtained for drying periods of 100 hours at a flow Reynolds number of 200. The results obtained under different environments indicate that solid dries faster in free convection environment when compared to forced convection situations.

NOMENCLATURE

C	concentration (kg/m ³)
C*	equivalent specific heat (J/kg K)
D	diffusion coefficient (m ² /s)
D _m	isothermal diffusion coefficient (m ² /s)
D _T	non isothermal diffusion coefficient (m ² /Ks)
H	enthalpy (J/kg); height(m)
k	thermal conductivity (W/mK)
U _∞	free stream velocity (m/s)
W	total moisture content (=w ₁ + w _v)
Re	Reynolds number (ρU _∞ H _b / μ)

Greek symbols

φ	relative humidity
β	coefficient of thermal expansion
β*	coefficient of expansion with concentration
ρ	mass density (kg/m ³)

Subscripts

b	brick
f	fluid or flow domain
l	liquid

o	dry porous solid
s	surface conditions
v	vapor
∞	ambient conditions

INTRODUCTION

Evaporating drying has an important application in drying of porous materials such as food stuffs, ceramic products, clay products, wood etc. to remove volatile liquid. But in the cases of preservation of food product and manufacture of ceramic products like bricks and tiles, drying phenomena are more complex because of their size and shape [1]. The conjugate heat and mass transfer from a solid body in a natural convection environment has many application in industry. Simultaneous heat and mass transfer through porous medium finds wide engineering applications such as drying, food processing, nuclear waster disposal etc.,. The drying of products such as tiles, bricks and electric insulators up to equilibrium moisture content is a critical process, as three types transport exist for liquid and vapour [2]. Industrial drying operations are based on heat transfer by convection, conduction and radiation or by combinations of these modes. In any transport modes the heat flow first reaches the clay body surface, and then penetrates inside. The drying of wet clay under constant temperature, air moisture and airflow takes place in three periods or stages [3]. The moisture movement within the solid during drying may be due to capillary forces during the constant rate drying period or due to diffusion during the falling rate period [4]. These different regimes of drying have been studied theoretically either using Luikov's model [5] which based on irreversible thermodynamics or Whitaker's continuum approach [1]. The drying of porous material has been studied using one-dimensional [6,7,8] and two-dimensional [9,10] models, using heat and mass transfer from the available correlation using boundary layer equations.

Since the actual process of drying is a conjugate problem, the heat and mass transfer, to and from the porous solid have to be studied along with the flow field. For natural convection of drying of wood as a conjugate problem, Zeghmati et al. [11] observed that the average Nusselt and Sherwood numbers are affected by internal diffusion of moisture within the solid. Conjugate analysis of drying [12,13,14] also shows that the drying behaviour differ from that obtained by decoupled analysis due to temperature and concentration non-homogenities at the solid-fluid

interface. In the previous work boundary layer type of equations are used for analysing the flow domain.

In the present work, two-dimensional Navier-Stokes equations have been solved for the flow field with additional buoyancy terms, resulting from temperature and concentration gradients during free and mixed convection environments, in the Y-momentum equation coupled with energy and moisture transport equations for the case of brick drying. Convective boundary conditions are imposed on top, left and right sides of the brick. The free, forced and mixed convection effects on drying behavior are analyzed. An interesting observation on temperature and moisture distribution within the solid and also along the solid surface are discussed.

GOVERNING EQUATIONS FOR THE FLOW FIELD

The two-dimensional Navier-Stokes equations, energy and the moisture transport equations are given by:

Continuity

$$\frac{\partial u}{\partial x} + \frac{\partial v}{\partial y} = 0 \quad (1)$$

X-momentum

$$\frac{\partial u}{\partial t} + u \frac{\partial u}{\partial x} + v \frac{\partial u}{\partial y} = -\frac{1}{\rho_f} \frac{\partial p}{\partial x} + \frac{\mu}{\rho_f} \left[\frac{\partial^2 u}{\partial x^2} + \frac{\partial^2 u}{\partial y^2} \right] \quad (2)$$

Y-momentum equation used during forced convection environment

$$\frac{\partial v}{\partial t} + u \frac{\partial v}{\partial x} + v \frac{\partial v}{\partial y} = -\frac{1}{\rho_f} \frac{\partial p}{\partial y} + \frac{\mu}{\rho_f} \left[\frac{\partial^2 v}{\partial x^2} + \frac{\partial^2 v}{\partial y^2} \right] \quad (3.1)$$

Y-momentum equation used during mixed and free convection environments

$$\frac{\partial v}{\partial t} + u \frac{\partial v}{\partial x} + v \frac{\partial v}{\partial y} = -\frac{1}{\rho_f} \frac{\partial p}{\partial y} + \frac{\mu}{\rho_f} \left[\frac{\partial^2 v}{\partial x^2} + \frac{\partial^2 v}{\partial y^2} \right] + g\beta(T - T_\infty) + g\beta^*(C - C_\infty) \quad (3.2)$$

where $g\beta(T - T_\infty)$ and $g\beta^*(C - C_\infty)$ are the buoyancy terms due to temperature and concentration differences respectively.

Energy equation

$$\frac{\partial T_f}{\partial t} + u \frac{\partial T_f}{\partial x} + v \frac{\partial T_f}{\partial y} = \frac{k_f}{\rho_f C_{pf}} \left[\frac{\partial^2 T_f}{\partial x^2} + \frac{\partial^2 T_f}{\partial y^2} \right] \quad (4)$$

Concentration equation

$$\frac{\partial C_f}{\partial t} + u \frac{\partial C_f}{\partial x} + v \frac{\partial C_f}{\partial y} = D \left[\frac{\partial^2 C_f}{\partial x^2} + \frac{\partial^2 C_f}{\partial y^2} \right] \quad (5)$$

GOVERNING EQUATIONS FOR THE POROUS SOLID

Using Darcy's law for capillary liquid mass flux and Fick's law for diffusive mass flux, the final form of energy and moisture conservation equations can be obtained in terms of the equivalent medium properties [5] in the form

$$\frac{\partial T}{\partial t} = K_1 \left[\frac{\partial^2 T}{\partial x^2} + \frac{\partial^2 T}{\partial y^2} \right] + K_2 \left[\frac{\partial^2 W}{\partial x^2} + \frac{\partial^2 W}{\partial y^2} \right] \quad (6)$$

where

$$K_1 = \left[\frac{k}{\rho_o C^*} + \frac{(H_v - H_l) D_{Tv}}{C^*} \right]; \quad K_2 = \frac{(H_v - H_l)}{C^*}$$

and

$$C^* = C_o + w_l C_l + w_v C_v$$

The moisture conservation equation can be written as

$$\frac{\partial W}{\partial t} = K_3 \left[\frac{\partial^2 W}{\partial x^2} + \frac{\partial^2 W}{\partial y^2} \right] + K_4 \left[\frac{\partial^2 T}{\partial x^2} + \frac{\partial^2 T}{\partial y^2} \right] \quad (7)$$

where

$$K_3 = (D_{mv} + D_{ml}); \quad K_4 = (D_{Tv} + D_{Tl})$$

(1) Boundary conditions used to solve governing equations in the flow field, during mixed and forced convection situations:

$$@ x = 0, u = U_\infty, v = 0, T = T_\infty, C = C_\infty \text{ for } 0 < y < H_f$$

$$@ x = L_f, \quad p = 0 \quad \text{for } 0 < y < H_f$$

$$@ y = 0, \quad u = v = 0 \quad \text{for } 0 < x < L_f$$

$$@ y = H_f, u = U_\infty, v = 0, T = T_\infty, C = C_\infty \text{ for } 0 < x < L_f$$

No slip boundary condition is prescribed on the solid surface.

(2) Boundary conditions used to solve governing equations in the flow field, during free convection flow situation:

$$@ x = 0, \quad u = 0 \quad \text{for } 0 < y < H_f$$

$$@ x = L_f, \quad u = 0 \quad \text{for } 0 < y < H_f$$

$$@ y = 0, \quad u = v = 0 \quad \text{for } 0 < x < L_f$$

$$@ y = H_f, \quad v = 0, T = T_\infty, C = C_\infty \text{ for } 0 < x < L_f$$

No slip boundary condition is prescribed on the solid surface.

(3) The boundary conditions at the air-porous solid interface are given as follows:

No slip

$$u = 0, v = 0$$

Temperature continuity :

$$T_f = T_s \quad (8)$$

Moisture continuity:

$$C_f = C(T, W)_s \quad (9)$$

Heat balance:

$$\begin{aligned} & \left[k + \rho_o (H_v - H_l) D_{Tv} \right] \frac{\partial T}{\partial n} + \rho_o (H_v - H_l) D_{mv} \frac{\partial W}{\partial n} \\ & = k_f \frac{\partial T_f}{\partial n} + (H_v - H_l) D \frac{\partial C_f}{\partial n} \end{aligned} \quad (10)$$

Species flux balance:

$$\rho_o \left[D_{Tv} \frac{\partial T}{\partial n} + D_{mv} \frac{\partial W}{\partial n} \right] = D \frac{\partial C_f}{\partial n} \quad (11)$$

Eqs. (6) and (7) represent the coupled transport equations for the solid. The top, left and right surfaces of the solid experiences the interface boundary conditions Eqs.(8) and (9), while the bottom surface is assumed to be adiabatic.

SOLUTION METHODOLOGY

Computational domain used during free convection environment is shown in Fig. 1. Air with a uniform free stream velocity of U_∞ is assumed to flow over a brick, during forced and mixed convection environments, placed on a flat surface as shown in Fig..2. The brick is assumed to be saturated with water. The temperature of the brick is less than that of air and the water evaporates from the brick due to the concentration difference between the brick surface and the ambient. This results in further reduction in the brick surface temperature. As drying proceeds with time, the solid reaches the wet bulb temperature corresponding to the given ambient conditions and remains at this temperature for a significantly long period of time. Finally, the brick gets heated up as heat flows from air to the brick. In drying process temperature and moisture variations affect both the temperature and moisture contents in the brick and the atmosphere adjacent to the solid surface. The Galerkin weighted residual method has been used to solve the governing equations for flow and solid domain. The flow equations are solved using Eulerian velocity correction method to obtain the velocities in the X-Y directions. Linear triangular elements are used to discretize the domain.

RESULTS AND DISCUSSIONS

The brick is assumed to be at an initial moisture content of 0.13 kg/kg of dry solid and temperature of 303 K. The drying medium is assumed to be same at 303 K with 50% relative humidity. During mixed and forced convection drying, air is assumed to be flow over a porous solid at a velocity of 1.8m/min (Re=200).

Comparison of temperature contours due to mixed and free convection drying(after 6 hours of drying) are shown in Fig. 3. Temperature contours are symmetric in nature during free convection drying. It is also

observed that drying is accelerated from left side due to mixed convection when compared to free convection, since gradients are high at the leading edge. During free convection, drying is more from right side when compared to mixed convection drying, since buoyancy forces have not been disturbed on the right side by external flow.

Temperature contours due to mixed and forced convection drying at Re = 200 (after 1 hour of drying) are compared in Fig. 4. It is observed that, due to buoyancy effects, solid dries earlier from all sides due to mixed convection when compared to forced convection. A comparison exercise of temperature and moisture contours was carried out at different hours of drying, since the drying rates are different during free, forced and mixed convection drying. For instance, after 6hours of mixed convection drying temperature in the brick varies from 296.14 to 297.48 K, whereas with forced convection drying it varies from 297.43 to 298.32 K and comparison at this hour did not show any physical variations between the two temperature contours. Hence temperature contours due to mixed and forced convection drying, at Re = 200, are compared after 1 hour. Moisture contours (after 12 hours of drying) due to mixed and free convection drying are shown in Fig. 5 while that due to mixed and forced convection drying are shown in Fig. 6. It shows the diffusion process is predominant in mixed convection when compared to other two.

Comparison of temperature variations with time at corner B (Figs. 1 and 2) of the solid due to mixed, forced and free convection drying are shown in Fig. 7. It is observed that temperature at the leading edge corner reaches a constant value (wet bulb temperature) approximately after 20, 25 and 60 hours respectively during mixed, free and forced convection drying.

Moisture content variations with time at location B of the solid due to free, mixed and forced convection drying are compared as shown in Fig. 8. It shows as discussed earlier that the moisture evaporation is more in mixed convection drying due to buoyancy effect and it is slow during free convection drying. During mixed convection drying, moisture content decreases from 0.13 to 0.06 kg/kg of dry solid whereas it decreases from 0.13 to 0.095 and 0.13 to 0.09 kg/kg of dry solid due to free and forced convection (Re=200) drying respectively. Also, the variation of moisture content, during forced and free convection drying, is almost constant except during initial hours of drying.

Comparison of heat and mass flux variations along the surfaces of the solid due to different convection process, after 115 hours of drying, are shown in Figs 9 and 10 respectively. It is observed that flux values are high along the surfaces of the solid during mixed convection drying compared to free and forced convection drying. In mixed convection drying at Re=200, the heat flux value at the leading edge corner B is about 40 W/m² after 115 hours of drying. This value is 30 W/m² and 10 W/m² for the same period of forced (Re=200) and free convection drying respectively. The mass flux values at location B are 1.7e-5 kg/m²s, 1.0e-5 kg/m²s and 3.0e-6 kg/m²s

respectively during mixed, forced and free convection drying.

Average moisture content variations in the solid with time are compared, during mixed, free and forced convection drying, as shown in Fig. 11. It is observed that average moisture content drops from 0.13 to 0.115, 0.112 and 0.094 kg/kg of dry solid due to forced, free and mixed convection drying respectively. This shows that rate of evaporation is high during mixed convection drying when compared to other two. Since the buoyancy forces dominate the flow field, at low Reynolds number, rate of evaporation is more during free convection when compared to forced convection drying. Also, up to 20 hours of drying, moisture content variations during mixed and free convection situations are similar. This may be due to undeveloped flow during mixed convection drying and buoyancy dominating during this period.

Comparison of drying rate variations with time, during free, mixed and forced convection environment, is shown in Fig 12. It is observed that at any instant of time, drying rate during mixed convection drying is high when compared to other two types of drying. Constant drying period can be observed during mixed convection drying. Drying rate increases during initial hours of free convection drying and then decreasing to approach the constant rate drying period.

CONCLUSIONS

Results obtained under different drying environments are compared with each other to show the importance of the buoyancy effects on drying process at $Re=200$. During this study, following observations have been listed for the conditions considered in the analysis:

- The conjugate mixed convection drying analysis predicts 30% more moisture evaporation from the solid when compared with forced convection drying.
- For the conditions considered in the present analysis, the solid reaches wet-bulb temperature after 60 hours of drying during forced convection, whereas it will take only 20 hours when buoyant forces are considered in the flow.
- During initial periods of drying, the solid dries faster in free convection environment when compared to forced convection situations.
- In mixed convection drying the heat flux value at the leading edge corner B is 70 W/m^2 , after 60 hours of drying. This value is 4 times higher when compared to forced convection drying at $Re=200$ and 2 times higher when compared to free convection drying. But, after 115 hours of drying, heat flux at the above location is 40 W/m^2 . It is 1.25 times higher when compared to forced convection drying and about 4 times higher when compared to free convection drying. This shows that the drying behavior is transient and fluxes increase or decrease at every instant of time.

- Temperature and moisture content distributions in the solid are not uniform due to front stagnation effect during forced and mixed convection drying.
- Rate of drying is higher at the leading edge in case of forced and mixed convection drying, since the gradients of temperature and moisture are higher in that location.

The above results indicate that it is essential to consider the buoyancy effects during forced convection drying analysis of brick.

REFERENCES

1. WHITAKER, S., (1977) A Theory of drying, *Advances in Heat Transfer*, 13, 119-203.
2. VERGNAUD, J.M., (1992) *Drying of polymeric and solid materials*, Springer-Verlag, London.
3. VINCENZINI, P., (1991) *Fundamentals of ceramic engineering*, Elsevier Applied Science, London.
4. PHILIP, J.R. and D.A. DEVRIES, (1957) *Trans. of American Geophysics Union*, 38, 222-232.
5. V.LUIKOV, (1966) Heat and mass transfer in capillary porous bodies, Pergamon Press, New York.
6. Ben NASRALLAH, S. and P. PERRE, (1988) *Int. J. Heat Mass Transfer*, 31, 297-310.
7. MURUGESAN, K., K.N. SEETHARAMU and P.A. Aswatha NARAYANA (1996) *Heat and Mass Transfer*, 32, 81-88.
8. KALLEL, F., N.GALANIS, B.PERRIN and R.JAVELAS, (1993) *J. Heat Transfer*, ASME Trans. 115, 724-733.
9. COMINI, G., and R.W.LEWIS, (1976) *Int. J. Heat Mass Transfer*, 19, 1387-1392.
10. FERGUSON, W. J. and R. W. LEWIS, (1991) Seventh Int. conference on Numerical Methods in Thermal Problems, Vol. VII, Part.2, 973-984, Stanford.
11. ZEGHMATI B., M. DAGUENET and G. LE PALEC, (1991) *International Journal of Heat Mass Transfer*, 34, 899-909.
12. DOLINSKY, A., S H. DORFMAN and B.V. DAVYDENKO, (1991) *Int.J.Heat Mass Transfer*, 34, 2883-2889.
13. MASMOUDI, W. and M. PRAT, (1991) *Int. J. Heat Mass Transfer*, 34, 1975-1989.
14. OLIVEIRA, L.S and K. HAGHIGHI, (1995) *Proceedings of 9th Int. Conference for Numerical Methods in Thermal Problems*, Atlanta, 80-88.

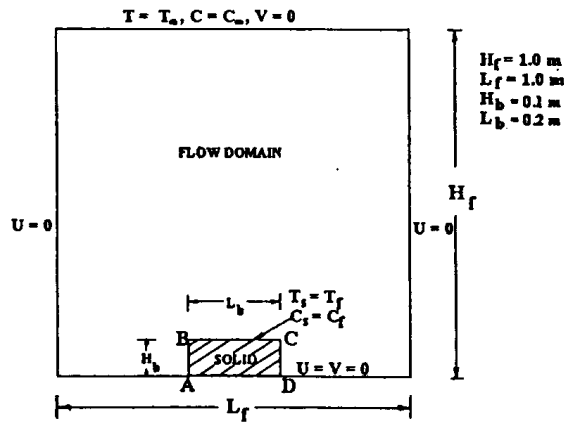


Fig. 1 Schematic diagram of computational domain (for free convection drying)

$H_f = 1.0$ m
 $L_f = 1.0$ m
 $H_b = 0.1$ m
 $L_b = 0.2$ m

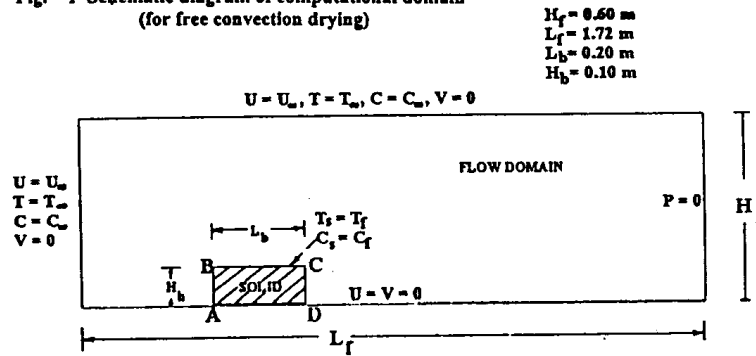


Fig. 2 Schematic diagram of computational domain (for forced and mixed convection drying)

$H_f = 0.60$ m
 $L_f = 1.72$ m
 $L_b = 0.20$ m
 $H_b = 0.10$ m

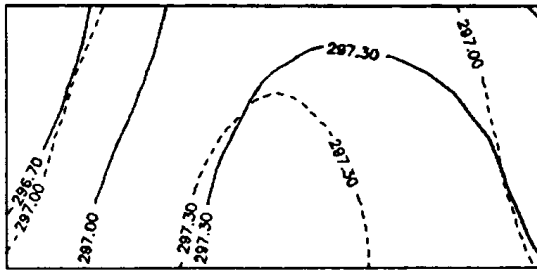


Fig. 3 Comparison of temperature contours in brick (mixed and free convection drying)

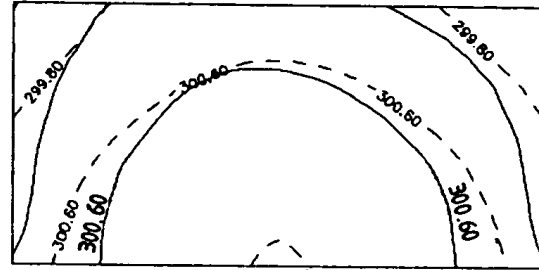


Fig. 4 Comparison of temperature contours in brick (mixed and forced convection drying)

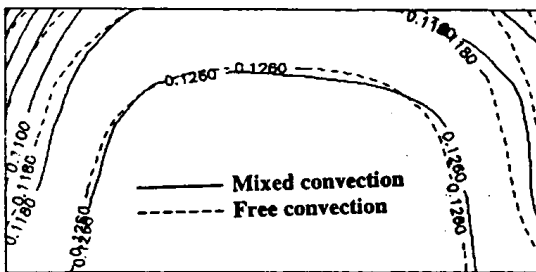


Fig. 5 Comparison of moisture contours in brick (mixed and free convection drying)

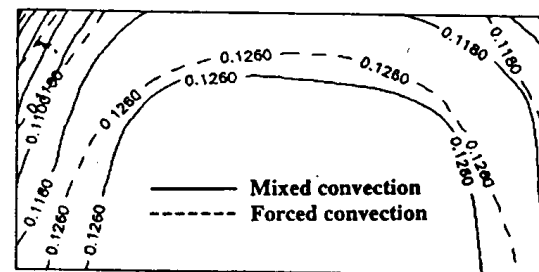


Fig. 6 Comparison of moisture contours in brick (mixed and forced convection drying)

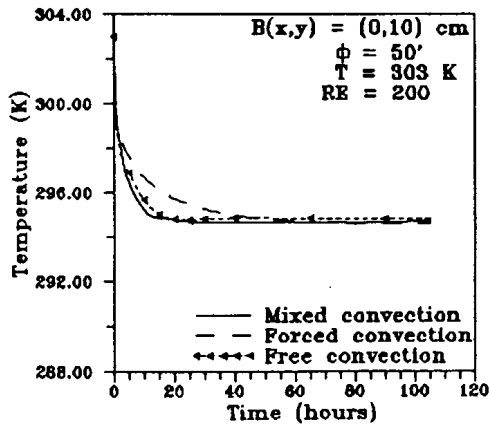


Fig. 7 Comparison of temperature variations with time

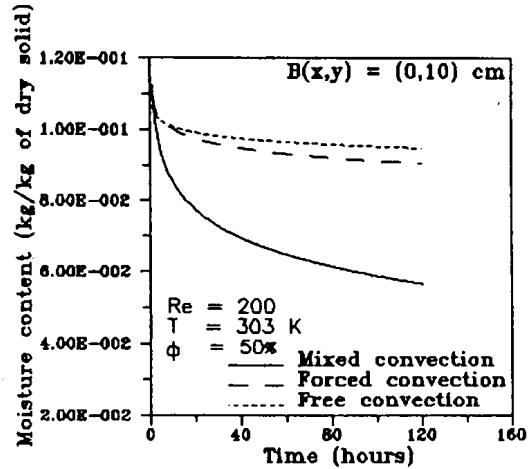


Fig. 8 Comparison of moisture content variations with time

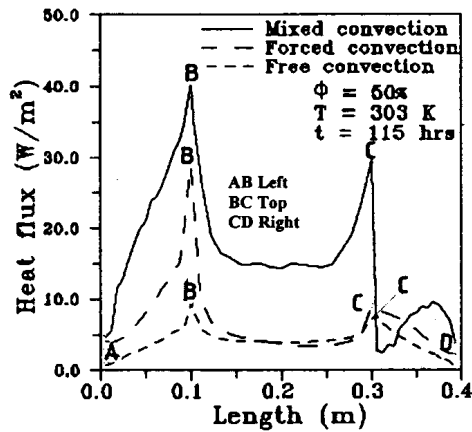


Fig. 9 Comparison of heat flux distributions along the surface of the brick

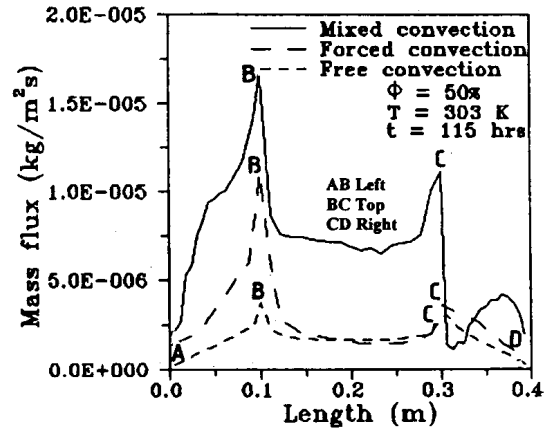


Fig. 10 Comparison of mass flux distributions along the surface of the brick

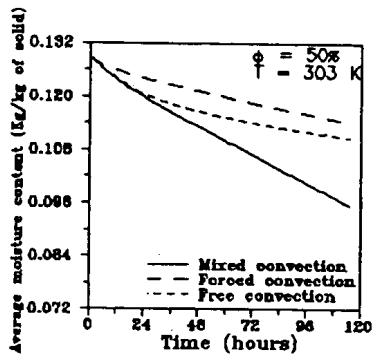


Fig. 11 Comparison of average moisture content variations with time

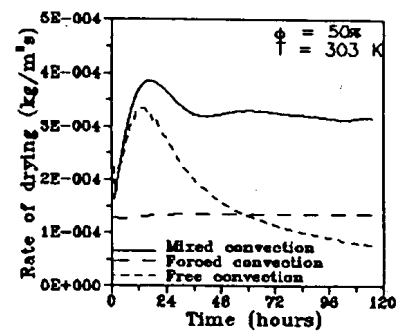


Fig. 12 Comparison of drying rate with time